

Graphene Nanomesh Transistors with high on/off ratio and good current saturation

S. Berrada, V. Hung Nguyen^{*}, A. Alarcón, D. Querlioz, J. Saint-Martin,
A. Bournel, C. Chassat and P. Dollfus
Institute of Fundametal Electronics, CNRS, Univ. of Paris-Sud, Orsay, France
^{*}L_Sim, SP2M, UMR-E CEA/UJF Grenoble 1, INAC, Grenoble, France
e-mail: salim.berrada@u-psud.fr

INTRODUCTION

Pristine graphene is a semimetal with excellent transport properties [1]. However, its gapless character limits the possible range of applications of graphene transistors (GFET), as it yields small on/off current ratio and poor saturation behaviour [2]. Bilayer graphene and graphene nanoribbons are graphene based materials that exhibit bandgap, but their use in GFETs remains a difficult task. In fact, bilayer graphene offers quite low bandgaps – around 130 meV [3] – and the fabrication of narrow-enough (sub-3 nm) ribbons with good edge roughness control remains challenging. Recently, the fabrication of graphene nanomesh (GNM) – a regular array of antidots separated by a sub-10 nm distance (see Fig. 1a) – has been reported [4]. Depending on the periodicity and the neck width of GNM lattice, bandgaps up to several hundreds of meV have been predicted to appear in large sheets of graphene [5,6]. Similar result can be obtained in superlattices of graphane-like islands formed by patterned adsorption of hydrogen atoms [7]. This kind of bandgap nanoengineering offers new possibilities to design improved devices delivering large currents [8].

MODEL, SIMULATED DEVICE AND RESULTS

In the present work, we investigate a GNM-based field-effect transistor (GNM-FET) by means of 3D numerical simulation. The model is based on the Green's function approach to solving a tight-binding Hamiltonian, self-consistently coupled to 3D Poisson's equation [9]. A 3D view of the simulated GNM-FETs is shown in Fig. 1b, with a gate length $L_G = 30$ nm and infinite width thanks to appropriate periodic boundary conditions along y direction. Comparison to a similar pristine graphene FET (GFET) is then provided.

The considered GNM has a bandgap of 508 meV, leading to an On/Off ratio as high as 1460 at $V_{DS} = 0.2$ V at room temperature. (Fig.2). We also note that increasing V_{DS} shifts the Dirac point (DP) toward higher V_{GS} for GNM-FETs while it is shifted toward lower V_{GS} for pristine GFETs, as shown in Fig. 3. This is due to the different conduction regimes that take place at DP for each device. The DP current (DPC) in pristine GFET results from the balance between the thermionic current and the chiral tunneling current through the gate-induced barrier [9]. In GNM-FET, the chiral tunneling is suppressed by the bandgap at DP. It can take place only at negative V_{GS} . The DP current is now resulting from the equilibrium between the thermionic current and the band-to-band tunneling current (BTBT). It is illustrated by the LDOS (for $k_y = 0$) and transmission at DP for $V_{DS} = 0.2$ V in Fig. 4. While at DP the chiral tunneling reduces when increasing V_{DS} in pristine GFET [9], the BTBT increases in GNM-FET. This explains why the DP moves differently as a function of V_{DS} . It is also remarkable that the GNM-FET provides a good saturation of current as a function of V_{DS} in the n-branch when the current is governed by the thermionic contribution. Indeed, thanks to the bandgap in the channel, the onset of BTBT is delayed to V_{DS} values higher than 0.5 V, which preserves a significant V_{DS} range of saturation.

We found the same behaviors for GNM-FETs with other neck widths and higher and lower energy gaps.

CONCLUSION

This work shows that well-designed GNM-FETs might offer both a high On/Off ratio and good saturation, making it a promising way to improve the operation of graphene based transistors.

REFERENCES

- [1] K.I. Bolotin et al., Solid-State Com 146 (2008) 351-355.
 [2] Ph. Avouris, Nano Lett. 10 (2010) 4285-4294.
 [3] J.B. Oostinga et al., Nat. Mater. 7 (2008) 151-157.
 [4] J. Bai, et al., Nat. Nanotechnol. 5 (2010) 190-194.

- [5] T.G. Pedersen et al., Phys. Rev. Lett. 100 (2008) 136804.
 [6] V. Hung Nguyen et al., J. Appl. Phys. 113 (2013) 013702.
 [7] R. Balog et al., Nature Mater. 9 (2010) 315-319.
 [8] V. Hung Nguyen, et al Nanotechnology 23 (2012) 065201.
 [9] A. Alarcon et al., IEEE Trans. Electron Devices, 60 (2013) 985-991.

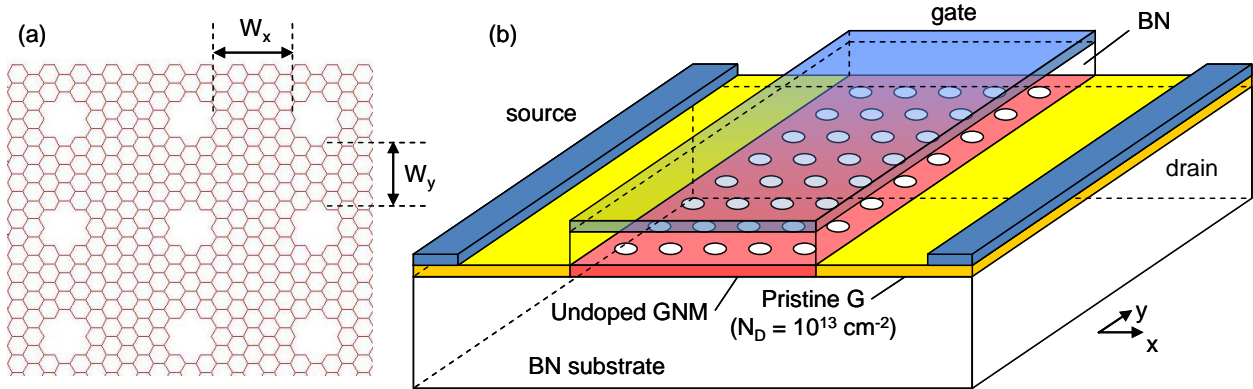


Fig. 1. (a) Typical view of a GNM lattice characterized by the neck widths W_x and W_y . (b) Schematic 3D view of the GNM-FET. The gate length is $L_G = 30 \text{ nm}$, the BN gate insulator thickness is 2 nm . The GNM neck widths are $W_x \approx 1.1 \text{ nm}$, $W_y \approx 0.9 \text{ nm}$.

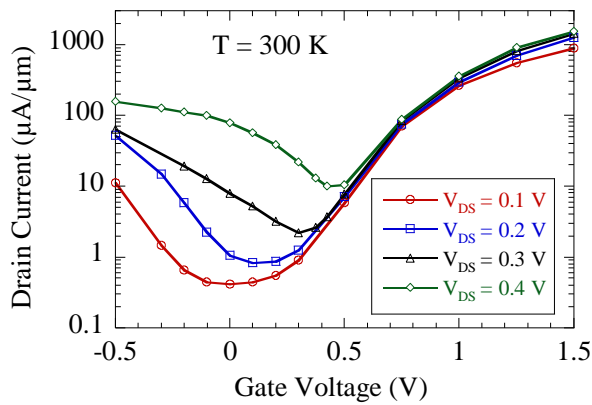


Fig. 2. Transfer characteristics of the GNM-FET.

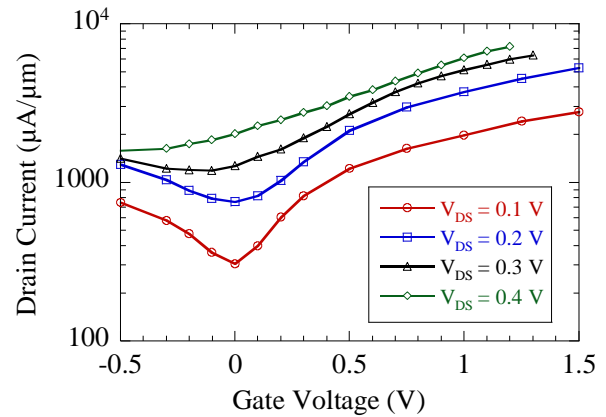


Fig. 3. Transfer characteristics of the Pristine GFET.

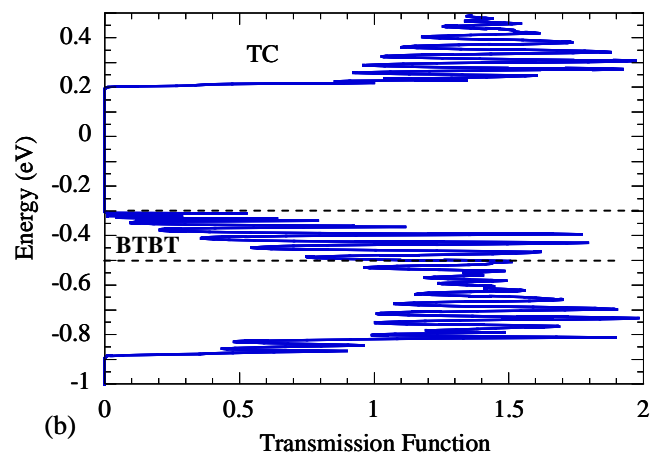
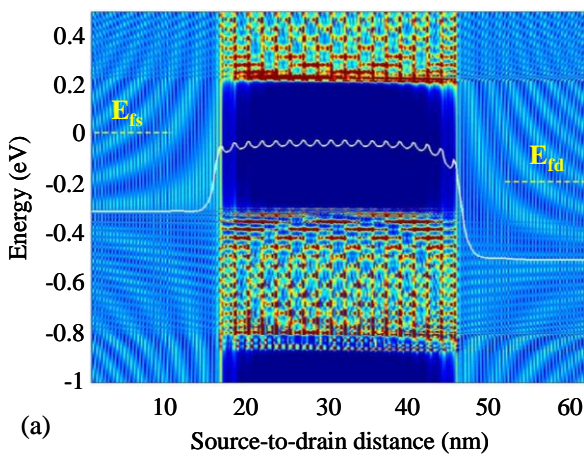


Fig. 4. (a) Local density of states for $k_y = 0$ in the GNM-FET for $V_{DS} = 0.2 \text{ V}$, $V_{GS} = 0.1 \text{ V}$ (Dirac point). The potential profile at the center of the device is superimposed (line). (b) Corresponding transmission function, with contributions of thermionic current (TC) and band-to-band tunneling (BTBT).